PROCEEDINGS OF ECOS 2022 - THE 35TH INTERNATIONAL CONFERENCE ON
EFFICIENCY, **C**OST, **O**PTIMIZATION, **S**IMULATION AND ENVIRONMENTAL IMPACT OF ENERGY SYSTEMS
1-3 JULY, 2022, COPENHAGEN, DENMARK

Remote ammonia production for the future energy demand of Belgium: Techno-economic optimization of local and remote ammonia production under uncertainty.

Kevin Verleysen[a,b], Diederik Coppitters[c], Alessandro Parente[b], Francesco Contino[c]

[a] Fluid and Thermal Dynamics (FLOW), Vrije Universiteit Brussels, Belgium, kevin.verleysen@vub.be, CA
[b] Aero-Thermo-Mechanical Department (ATM), Université Libre de Bruxelles (ULB), Brussels, Belgium
[c] Institute of Mechanics, Materials and Civil Engineering, Université Catholique de Louvain, 1030 Louvain-la-Neuve, Belgium

Abstract:

Regions with abundantly available renewable energy are not necessarily the same as those with a high population density and high energy consumption. Therefore, renewable energy can be produced in optimal climate conditions with a remote renewable hub and transported to these population-dense regions. To establish this energy transport, ammonia provides a flexible, easy-to-handle energy carrier, which already showed a viable option for transporting energy from Australia to Japan. However, current literature rarely considers the impact of techno-economic uncertainty on the feasibility of this transport. Therefore, we performed a robust design optimization on the levelized cost of ammonia and the power-to-ammonia efficiency considering techno-economic uncertainties. Furthermore, we compared the local (Belgium) and remote (Morocco) ammonia production and transport for Belgium. This paper provides the robust designs (i.e. least sensitive to uncertainty) for local and remote renewable ammonia production, the advantages of both approaches on the levelized cost and power-to-ammonia energy efficiency. The results confirm that ammonia production in regions with high solar irradiance following the convenient transport of ammonia is cost-effective and robust (790 euro/tonne$_{NH_3}$ in mean and 128 euro/tonne$_{NH_3}$ in standard deviation) over local production (1334 euro/tonne$_{NH_3}$ in mean and 249 euro/tonne$_{NH_3}$ in standard deviation) to the higher available solar irradiance. The local production provides for higher and robust Power-to-ammonia energy efficiencies (53.6% in mean and 0.1% in standard deviation), while the remote production is less efficient and more sensitive to uncertainties (47.9% in mean and 1.53% in standard deviation). Both objectives are highly influenced by the capacity of the photovoltaic arrays and the electrolyzers, where in the case of Morroco, the fuel cell capacity plays a major role in the efficiency of the system. Future work aims to perform a techno-economic-environmental evaluation of this robust design optimization, including environmental indicators like recycling of composite materials and depletion of rare materials.

Keywords:

Power-to-ammonia, Haber-Bosch Synthesis, Robust design optimization, Levelized cost of ammonia.

1. Introduction

Ammonia (NH_3) as an energy carrier boomed in recent years because it can support the defossilisation of the world. The need to produce this fuel in large mass is becoming increasingly important to transport renewable-based hydrogen (produced by renewable-powered electroyzers) over large distances while advancing from a fossil-fueled production of nitrogen fertilizers to renewable ones [1–4]. Ammonia has a wide range of applications similar to that of renewable hydrogen. Studies show the potential of ammonia as a maritime fuel or in the power industry (with gas turbines) [5]. Projects across the world (between Japan and Australia, in Germany and in Korea) examine the advantage of renewable ammonia and its possibility to transport this energy vector via ship or pipelines to other countries or continents in the future [6]. Where, for instance, the consortium with Australian and Japanese member industries want to establish the production and transportation of cheap renewable ammonia from energy rich location to high demand locations. Other projects are looking for ways to use this ammonia as a direct or indirect fuel for producing electricity [5]. For the case of Belgium, renewable energy sources are scarce compared to other regions in Europe with higher wind speed (north of Scotland) and solar irradiance (south Europe) [7], therefore Belgium can not rely on only domestic renewable energy supply in the future [8]. The study of Limpens et al. [9] already showed the drive towards Power-to-Gas systems to compensate for the need of seasonal storage and flexibility in a low-CO_2 emission society. The hydrogen import coalition [10] showed the economic feasibility of importing renewable energy to Belgium over sea through the use of energy carriers. These energy carriers included hydrogen, ammonia, methane, methanol and liquid organic hydrogen carriers, where producing ammonia and methanol in Chile, Oman and Morocco were com-

petitive against different hydrogen production sites in Belgium. Another advantage for considering import over local NH_3 production is the additional electric load on the electricity grid when renewables are not sufficient to cover the PtA system base load [11]. Although this local production would be favorable because there is no need for large distance transport, PtA plants in northern Africa can be beneficial because of the ideal location in terms of availability of water and high total global solar irradiance (2303.5 kWh/m^2/y), than in Belgium (population dense coast and low annular global solar irradiance (1101 kWh/m^2/y) [2, 6, 12].

Traditionally, ammonia is produced by a Steam Methane Reforming (SMR) process to form hydrogen from methane while emitting CO_2. The hydrogen gas is mixed with nitrogen (obtained from the air) and provided to the Haber-Bosch Synthesis (HBS) process where the mixture is synthesized at high pressure and high temperature to ammonia over a metal catalyst [13]. This process has technologically improved (in terms of energy efficiency and reactor design) and commercially matured over the last 100 years to sustain the high demand of ammonia as a fertilizer at a low cost [14]. Currently, the transition from these fossil-fueled Haber-Bosch plants to the PtA plant is promoted to reduce the global carbon footprint of the nitrogen fertilizer and to be used for the future energy demand [14–16]. The traditional HBS process is adapted to operate at a steady-state condition at its nominal level. Without an unadapted Haber-Bosch process, these PtA plants would require in practice large hydrogen tanks and a back-up system to continue the HBS to operate at the same load when there is not enough renewable energy available in islanded locations [6, 17, 18]. The patent of Ostuni et al. [19] showed the capability to regulate the load of a traditional and renewable-based ammonia synthesis loop by controlling the inert gas concentration and purge flow rate of the process, which allowed to reduce the minimal load between 10% to 20% from the nominal load. The research of Cheema et al. [20] demonstrated also this capability but added the flexibility under variable loads with an adapted ammonia reactor designs. Cheema et al. [20, 21] concluded that changing the inert feed concentration, feed flow rate and the H_2/N_2 ratio to the process create the highest flexibility for the PtA process to operate when powered by renewables. Beerbühl et al. [22] developed a heuristic optimization approach to integrate renewable energies through the optimal sizing and scale of the chemical processes. The study applied this heuristic approach on a non-linear ammonia synthesis process and established the necessity of using non-linear modeling for the optimized scheduling and capacity planning of these hydrogen-based storage facilities. Other papers as the one of Nayak-Luke et al. [17, 23] and Palys et al. [24] show especially how this scheduling and advanced power management strategies provide for lower Levelized Cost of Ammonia (LCOA) by minimizing the H_2 and N_2 buffer tank capacity. In particular, the study of Nayak-Luke et al. [17] presented the cost competitive location in the future (2030) by adopting this strategic scheduling in combination with a reduction of cost (levelized cost of electricity and capital expenses of the electrolyzer). In this report, some of the locations in Europe can only compete with other locations (outside Europe), when the electrolyzer's full load hours are over 5000 h, while in Northern-Africa, the electrolyzer only need a full load hour between 2500 h and 3000 h to achieve the same levelized cost (below 450 USD/tonne$_{NH_3}$) [17]. However, these studies do not consider uncertainties related to changes in cost and energy consumption while optimizing the design of such energy capture systems. These uncertainties lead to a reduction in production and revenue over time. Therefore, robust designs are needed to reduce the sensitivity of these uncertainties (technical and economical) and quantify the effect of these uncertainties on certain technical or economic objectives [25].

In this paper, we optimize the energy efficiency, levelized cost of NH_3 and their sensitivity against uncertainties of a photovoltaic-powered grid-connected PtA plant in Belgium and an isolated photovoltaic-powered PtA plant in Morocco where ammonia is transported via ship to Belgium. Within this study, we disregard the reconversion of this ammonia back to hydrogen or electricity and assume that the ammonia can be used in the power industry or in the fertilizer industry. The optimizer determines the size of all individual components (PhotoVoltaic (PV) array capacity, the electrolyzer capacity, the back-up system, the storage tanks, and HBS capacity) and power flows to maximizing the mean PtA energy efficiency while minimizing the mean LCOA while minimizing the sensitivities of uncertainties on these objectives.

2. Methodology of the stand-alone power-to-ammonia plant

In this section, we describe first the global PtA model including the individual components. Next, the climate data and the objectives are defined. Afterwards, the model uncertainties that are affecting the system performance and cost are presented. Finally, the robust design optimization method where we combine a metaheuristic optimizer and uncertainty quantification analysis method is described.

2.1. Model description

The stand-alone PtA model can be disassembled into five main parts (Figure 1). The first part is the conversion from solar irradiance to electric energy using PhotoVoltaic (PV) cells. The second part is where a section of this electric energy is used to produce hydrogen and nitrogen, respectively using a Proton Exchange Membrane (PEM) electrolyzer and an Air Separation Unit (ASU) unit. When the power to the electrolyzer exceeds its capacity, the excess is provided to the ASU. When this power again exceeds to capacity of the ASU, this

residual power is discarded. The third section is where the hydrogen and nitrogen gas are intermediary stored in buffer tanks. A fuel cell stack or grid connection or both powers the ammonia process when there is not sufficient power available to compensate for a set load. In the forth section, hydrogen and nitrogen are extracted from the tanks and provided to the Haber-Bosch to produce ammonia. The Haber-Bosch itself is directly powered by the PV panels or by the backup system (grid and/or fuel cells). In the last section, the produced ammonia is shipped when the PtA plant is located in Morocco. The full PtA plant and ship model are developed in Python which are described in the following subsections.

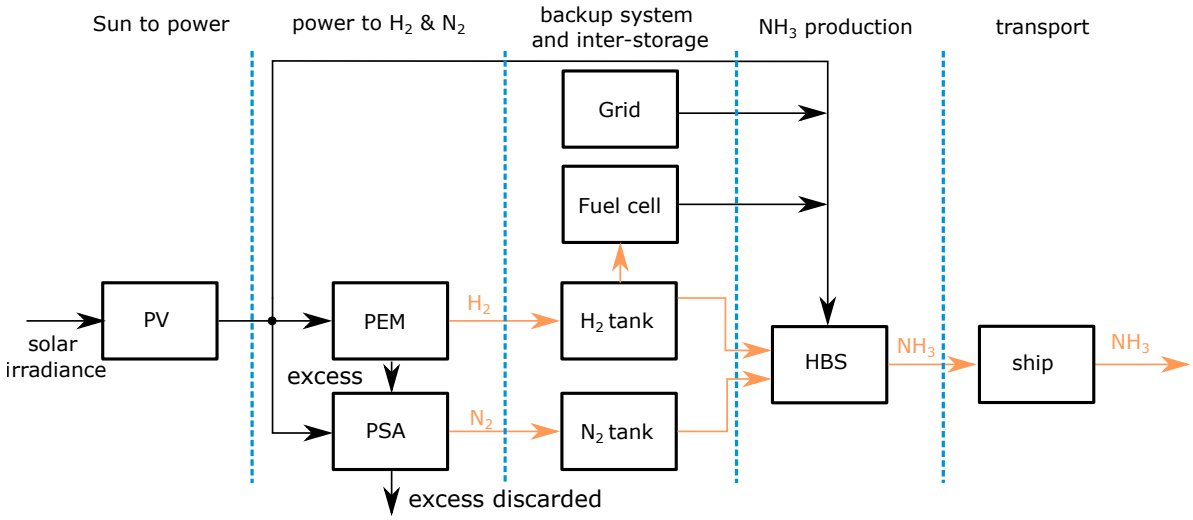

Figure 1: The flow chart of the Power-to-Ammonia plant where the plant is subdivided in five groups. The photovoltaic cell convert the solar irradiance in electric power. This power is distributed over the production of hydrogen, nitrogen and ammonia. The intermediate storage buffers the hydrogen and nitrogen gas and a backup system provides power to the Haber-Bosch when there is insufficient solar power. In the case of the Moroccan PtA plant, a ship transports (and partially use) the ammonia to Belgium.

2.1.1. Photovoltaic cells

To determine the electricity produced by a PV array, we imported the model from the *PVlib* Python library [26], which has been validated with experimental data and commercial software [27]. The model quantifies the PV panel power production through a current-voltage characteristic:

$$I_{\mathrm{PV}} = I_{\mathrm{L}} - I_0 \left(\exp\left(\frac{U + IR_{\mathrm{s}}}{n_{\mathrm{diode}} N_{\mathrm{s}} U_{\mathrm{th}}} \right) - 1 \right) - \frac{U + IR_{\mathrm{s}}}{R_{\mathrm{sh}}}, \tag{1}$$

for which the parameters are derived from manufacturer data [28]. We adopted the characteristics of a monocrystalline silicon PV panel (Sunpower SPR X-19-240-BLK) [29] as a reference for the operation a the PV array.

2.1.2. Proton exchange membrane electrolyzer and hydrogen tank

We adopted a PEM electrolyzer, as the technology promises a fast response time ($<$1 second) and full operational flexibility. These characteristics are crucial when coupled to an intermittent renewable energy supply [30]. The hydrogen production of a PEM electrolyzer is directly related to the operating current:

$$\dot{n}_{\mathrm{H_2}} = \frac{I_{\mathrm{PEM}}}{2F}. \tag{2}$$

To derive the operating current from the applied electric power, we adopted the voltage-current characteristic from Abdin et al. [31]. The operating current considers the open-circuit voltage U_{oc}, activation overpotential U_{act}, ohmic overpotential U_{ohm} and concentration overpotential U_{con}, which depend, among others, on the operating temperature, pressure and current:

$$U_{\mathrm{PEM}} = U_{\mathrm{oc}} - U_{\mathrm{act}} - U_{\mathrm{ohm}} - U_{\mathrm{con}}, \tag{3}$$

We refer to Abdin et al. [31] for the details on the quantification of these overpotentials.

The produced hydrogen is then stored in a hydrogen tank where the sizing of the tank needs to be minimized by the optimizer as is described by Nayak-Luke and Bañares-Alcántara [17]. A minimum capacity of 10% is adopted to allow a maximum depth of discharge of 90% as described by Wang et al. [32]. No pressure and mass losses are considered inside the tank.

2.1.3. Air separation unit and nitrogen tank

The Air Separation Unit (ASU) generates nitrogen gas obtained from the air. Three systems could perform this operation at various scales. The first type of system adsorbs with a membrane the nitrogen from the air based on selective permeation [33]. This technology is seen as cost-effective for the support of the Haber-Bosch in small-scale operation (below 150 ton_{NH_3}/day) [34]. Sanchez et al.[34] showed the cost-competitiveness of a second ASU system, the Pressure Swing Adsorption (PSA) below this production limit of 300 ton_{NH_3}/day. Above this limit, the modular design of the PSA becomes less attractive in terms of production and investment cost and nitrogen purity, where a distillation column (liquefying the nitrogen in the air) becomes more favourable for large scale production. The energy efficiencies of these three air separation systems vary over a specific range. Based on five papers [17, 23, 24, 35, 36], we observed the range of an ASU energy efficiency lies between 0.108 kWh/kg_{N_2} and 0.243 kWh/kg_{N_2}. Therefore, we implemented a linear relationship between the nitrogen gas production (in kg/h) and the hourly electric energy consumed by the ASU with an uncertain energy efficiency between these boundaries.

The produced nitrogen is then assumed to be stored in a nitrogen tank. Like in the case of the H_2 tank, the optimizer needs to minimize the maximum capacity of the nitrogen tank (in kg) as is described by Nayak-Luke and Bañares-Alcántara [17]. We assume the same maximum depth of discharge of the hydrogen tank, where we considered a minimum capacity of 10% and no pressure and mass losses inside the tank.

2.1.4. Haber-Bosch synthesis process

The Haber-Bosch (HB) process synthesizes the hydrogen and nitrogen gas with a catalyst to ammonia. The efficiency of this synthesis loop depends on various operating conditions and design parameters, e.g. the loop pressure (ranges between 100 bar and 250 bar), the temperature inside the ammonia reactor (reaching between 350°C and 550°C), the catalyst material, the type of separation process (via a condensation or pressure swing adsorption system) and the reactor configuration (direct or indirect cooling). This combination of elements and the capacity of the ammonia synthesis system results in different energy efficiencies for the Haber-Bosch process (between 0.532 kWh/kg_{NH_3} and 0.648 kWh/kg_{NH_3}) [17, 18, 23, 37]. We integrated a linear relation between the ammonia production (in kg/h) and provided electric energy with an (uncertain) energy efficiency to model the HB process. We assume the process will constantly operate at a H_2/N_2 ratio of 3:1. So for each produced kg of ammonia, 14/17 kg of N_2 and 3/17 kg of H_2 gas are removed from their respective storage tanks. In addition, the load can only increase with steps of 20%/h between a designed minimum load and 100%. When the power to the HB is larger than 20% of the previous load, the load will increase by 20%. When the load is lower than 20%, the load will decrease by 20%. In addition, when the N_2 or H_2 buffer tanks are operating at their minimum (maximum) capacity, the NH_3 production will be decreased (increased). The ammonia production will be adapted to allow the buffer tanks to recover from their boundary levels. For example, when the buffer tanks reaches their maximum capacity, a higher ammonia production during the night will occur or when the buffer tanks reaches their minimum capacity, the ammonia production will be minimized during the day. This load scheduling shows better performance in overall efficiency and levelized cost, to the decreasing dependency of grid or large back-up systems in combination with the high storage cost of hydrogen [23, 38].

2.1.5. Backup system

We incorporated a backup system to accommodate a steady power supply to the Haber-Bosch process when there is insufficient electric power, e.g. a sudden decrease in solar irradiance or powering the Haber-Bosch during the night. This backup system could be provided in two ways: a dispatchable grid or a fuel cell stack. For the case of Belgium, we assume there is a power grid available at all times, like in the case of Armijo and Philibert [18]. In addition, a fuel cell can be installed to reduce the PtA dependency on the grid, which is done in the study of Palys et al. [38]. For Morocco, we assume this plant will be grid-isolated and fully backed up by a fuel cell-based system like in Nayak-Luke et al. [23]. Whenever there is no grid and the backup capacity is not sufficient to support the Haber-Bosch process at a particular hour, the ammonia production is set to zero for that hour.

The PEM fuel cell is characterized similarly to the PEM electrolyzer. The voltage-current characteristic is adopted from Murugesan et al. [39], which has been validated on the Ballard-Mark-V PEM fuel cell:

$$U_{\text{PEMFC}} = U_{\text{Nernst}} - U_{\text{act}} - U_{\text{ohm}} - U_{\text{con}}. \tag{4}$$

We refer to the work of Murugesan et al. [39] for the detailed quantification of these overpotentials.

2.1.6. Ship model

A ship transports ammonia from Morocco (Aglou) to Belgium (Zeebrugge). We adopted the ship model of Kim et al. [40], which is operating by an ammonia-based engine propulsion system. The reported ship has a maximal capacity of 500 reefers, which are refrigerated containers with a volume of 28.3 m^3. We assumed the

transported ammonia is stored at a pressure of 11 bar and 27°C, having a density of 600 kg/m^3. We integrated the same ship model (Case 2 of [40]) and its load profile while including the economical parameters of the ship's components. The study reported a daily fuel consumption of 69.9 tonne$_{NH_3}$ with 250 reefers, which could transport 4290 tonne NH_3 with each trip in our case. However, we adapted the electric service profile of the ship with a linear scaling factor. This scaling factor allows the optimizer to design the total reefer capacity of the ship. So a more significant amount of reefers on the ship can transport more NH_3 but increase fuel consumption. When the number of reefers is relatively small, less NH_3 is transported, but the fuel consumption will be less (21.6% less fuel consumption between the minimum and maximum capacity of reefers). Based on the maximum speed of the ship (a maximum speed of 19 knots [40]), we determined with a tool [41] that the ship will travel between 3 and 4 days from Aglou to Zeebrugge.

2.2. Climate data

As climate data, we provide the hourly ground solar irradiance and ambient temperature of the year 2019 of Belgium (Zeebrugge) and Morocco (Aglou) to the PV-powered PtA plant (Figure 2) [42]. We observe a significant difference of 41.8% in the yearly solar irradiance in the two locations. The location in Morocco (Aglou) shows a more stable solar irradiance over the year, whereas the solar irradiance in Belgium (Zeebrugge) is more affected by the weather and seasons.

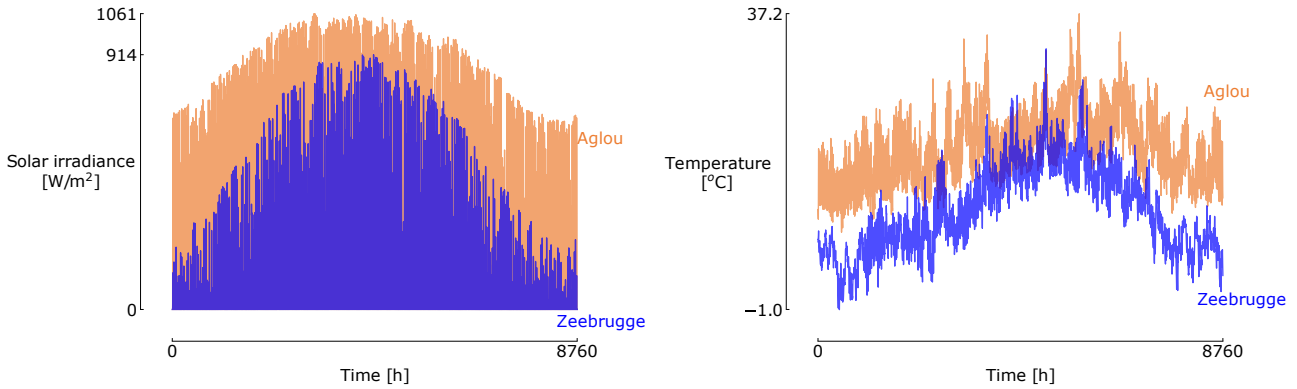

(a) Ground-level solar irradiance data of Zeebrugge (Belgium) and Aglou (Morocco) of 2019.

(b) Temperature data of Zeebrugge (Belgium) and Aglou (Morocco) of 2019.

Figure 2: Climate data of Zeebrugge (Belgium) and Aglou (Morocco) of 2019 [42].

2.3. Objectives

The main objectives of this paper are to maximize the total energy efficiency of the PtA plants (η_e) and the Levelized Cost of Ammonia (*LCOA*) while minimizing their sensitivity against uncertainties. We defined this energy efficiency as the ratio of the total ammonia production and the total amount of energy (E_{total}) provided to the system. This total energy is composed of two parts: the energy provided to the system via the PV panels (E_{PV}) and the energy supplied by the grid (if the grid is available). To minimize the excessive hydrogen and nitrogen production, we subtract the energy stored in the H_2 and N_2 tank. The energy efficiency of the PtA plant design is therefore defined as follow:

$$\eta_e = \frac{m_{\text{NH}_3} \cdot \text{LHV}_{\text{NH}_3} - |E_{\text{H}_2,\text{tank}}| - |E_{\text{N}_2,\text{tank}}|}{E_{\text{PV}} + |E_{\text{grid}}|} \quad [\%], \tag{5}$$

where m_{NH_3} amount of ammonia produced over the year in kg, LHV is the Lower Heating Value of ammonia (18.6 MJ/kg$_{\text{NH}_3}$), E_{H_2} and E_{N_2} are the energy in the hydrogen and nitrogen tank at the end of the year, E_{PV} is the electric energy produced by the solar panels and E_{grid} is the grid energy in MJ. The nitrogen energy is calculated based on the uncertain energy efficiency, where the energy required to produce or compensate for the consumed nitrogen is determined. As our second objective, we want to minimize the levelized cost of ammonia. The *LCOA* is defined as:

$$LCOA = \frac{\sum_i \left(CAPEX_{a,i} + OPEX_{a,i}\right) + C_{\text{grid}}}{m_{\text{NH}_3}} \quad [\text{euro/tonne}_{\text{NH}_3}] \tag{6}$$

In this equation, the *LCOA* depends on the total annualized investment cost ($CAPEX_{a,i}$) and annualized operational cost ($OPEX_{a,i}$) of the component i, the grid cost (C_{grid}) and the yearly ammonia production (m_{NH_3}). We implemented the method of Zakeri and Syri [43] to convert the capital expense (*CAPEX*) of a component i to

its annualized investment cost ($CAPEX_{a,i}$). The *CAPEX* of each component depends on the installed capacity. We considered a 30 year lifetime for the PtA plant and ship [17, 18], used an interest rate of 4%, an inflation rate of 2% and a grid price of 71.5 euro/MWh [44].

2.4. Design space and uncertainty characterization

The PtA system is sized according to a set of design variables to minimize the levelized cost and maximize the system's efficiency. We selected in total 11 design variables that influence these objectives (Table 1). From these 11 design variables, eight design variables are used for sizing an individual component, i.e. the PV array capacity size, the PEM and FC stack size, the maximum capacity of the HBS process, the H_2 and N_2 tank capacity and the number of reefers. The residual three design variables are dedicated to the power distribution to the PEM stack and the HB process and determining the optimal minimal load of the Haber-Bosch process.

Table 1: Decision variables of the NSGA-II algorithm.

Decision variable	Minimum	Maximum	Unit
PV capacity	0	10^6	[kWp]
PEM capacity	0	10^6	[kW]
FC capacity	0	10^5	[kW]
HBS capacity	0	10^5	[kW]
ASU capacity	0	10^5	[kW]
H_2 tank	1	10^5	[kg]
N_2 tank	1	10^5	[kg]
reefer	1	500	[-]
fraction P_{PV} to P_{HBS}	1	20	[%]
fraction P_{PV} to P_{PEM}	80	99	[%]
HBS minimal capacity	10	50	[%]

We identified 19 uncertainties divided into 14 economic and 5 technical uncertainties for the uncertainty characterisation. We extracted economic values from PtA studies and converted the reported currencies to $euro_{2022}$. The range of each component is then determined and used as an uncertainty (Table 2). For the four technical uncertainties, we implemented the energy efficiency ranges of the Haber-Bosch and the air separation and the solar irradiance and temperature of both locations. We based the uncertainty of the solar irradiance and temperature for these locations on weather data of 11 years (between 2005 and 2016) [45]. In Aglou (Morocco), we observed a relative standard deviation on the yearly global irradiance and temperature of 3.11% and 14%, whereas in Zeebrugge, these are 4.19% and 58%. In addition, the time that the ship spends to go from one port to another is also taken uncertain (between 3 and 4 days). We consider all (technical and economic) uncertain parameters as Uniform distributions except for the solar irradiance and temperature; we consider them as Gaussian distributions.

Table 2: Economic uncertainty ranges of the capital and operational expenses of components of the Power-to-Ammonia plant, where the reported currencies are converted into $euro_{2022}$.

Component	*CAPEX*			*OPEX*			Sources
	Minimum	Maximum	Unit	Minimum	Maximum	Unit	
PV	350	921	euro/kWp	0.01	0.03	%*CAPEX*/y	[17, 18, 24, 44]
PEM	482	1223	euro/kW	0.01	0.03	%*CAPEX*/y	[6, 17, 18, 24, 46]
HBS	455	5317	euro/kW	0.01	0.03	%*CAPEX*/y	[18, 24, 46]
ASU	1391	7162	euro/(kg/h)	0.01	0.03	%*CAPEX*/y	[17, 18, 24, 47]
FC	921	2400	euro/kW	0.01	0.03	%*CAPEX*/y	[17, 18, 24, 44]
H_2 tank	189	1420	euro/kg	0.01	0.03	%*CAPEX*/y	[17, 18, 24, 48]
N_2 tank	19	19	euro/kg	0.01	0.03	%*CAPEX*/y	[24]

2.5. Robust design optimization

A meta-heuristic optimizer is implemented to find this set of optimized design variables. However, to the uncertain (technical and economic) parameters, we need to quantify the sensitivity of the objectives by these parameters with an Uncertainty Quantification (UQ) analysis. Then, we can optimize the uncertain objectives according to their statistics (mean and standard deviation). This methodology to optimize the design of a system according to an uncertain objective is called Robust Design Optimization (RDO) [28, 44, 49, 50]. We implemented the Non-dominated Sorting Genetic Algorithm II (NSGA-II) to optimize the objectives by finding

Table 3: Technical uncertainties of the Power-to-Ammonia plant.

Component	Minimum	Maximum	Unit	Source
Specific energy consumption HBS	0.532	0.648	kWh/kg	[17, 18, 23, 37]
Specific energy consumption ASU	0.108	0.243	kWh/kg	[17, 23, 24, 35, 36]
Solar irradiance Belgium	-4.19	4.19	%	[45]
Solar irradiance Morocco	-3.11	3.11	%	[45]
Temperature Belgium	-0.589	0.589	°C	[45]
Temperature Morocco	-0.145	0.145	°C	[45]
Shipping day (one trip)	3.0	4.0	days	[41]

the optimized set of decision variables. This set corresponds to the design samples that dominate every other sample in at least one objective, resulting into a Pareto set of design samples. For the UQ analysis of static deterministic models, Monte Carlo simulation is commonly used but takes up to 10^6 evaluations to get accurate statistics of the mean, variance and higher-order moments [51–53]. For this reason, we adopted the Polynomial Chaos Expansion (PCE) where the number of evaluations is reduces while creating a meta-model from orthogonal polynomials and their corresponding polynomial chaos coefficients, as is described by Blatman and Sudret [54]. We refer to the work of Coppitters et al. [28, 44, 50] for further details of the implemented RDO algorithm.

3. Results and discussion

We discuss first the results of the design optimization (with and without uncertainties) and compare the deterministic and robust design cases. Finally, we discuss and compare the key design variables of the Moroccan and Belgian PtA process.

We choose a population size of 30 and 300 generations as the computational budget for each design optimization. We selected a polynomial order of 2 for the PCE algorithm in the RDO case. The deterministic design optimization (where we excluded the uncertainties on the parameters) resulted for each case in a Pareto front (Figure 3a). We observe that the Belgian case can attain higher energy efficiencies than the Moroccan case but at significantly higher costs (4035 euro/tonne$_{NH_3}$ with an efficiency of 55.4%). The Moroccan case attains the highest efficiency at 50.6% at a cost of 1938 euro/tonne$_{NH_3}$. This efficiency difference between these two points is related to the backup system (fuel cell stack) and transport of NH_3, where both systems cannibalizes fuel (H_2 or NH_3) to power the plant during the night or the ship during transport. When comparing the levelized cost of NH_3, the Moroccan plant can achieve a lower *LCOA* at a higher efficiency (708 euro/tonne$_{NH_3}$ and 46.3%) than the Belgian plant (1114 euro/tonne$_{NH_3}$ at 45.3%). These *LCOA* values are comparable to the ones found in the paper of Nayak-Luke and Bañares-Alcántara [17]. In this case study, the *LCOA* of Morocco was 751 euro$_{2022}$/tonne$_{NH_3}$ (757 USD$_{2020}$/tonne$_{NH_3}$) while in Belgium this cost lies between 731 and 1258 euro$_{2022}$/tonne$_{NH_3}$ (between 737 and 1269 USD$_{2020}$/tonne$_{NH_3}$). The difference between the paper [17] and ours (besides the difference in technical and economic parameters) is the inclusion of wind power, location-dependent discount rates and excluding the shipping cost to deliver NH_3 to Belgium. However in the lowest *LCOA* case, the inclusion of the ship is minimal in cost (1% of the component cost) and in NH_3 consumption (ship cannibalizes 6.55% of the produced NH_3).

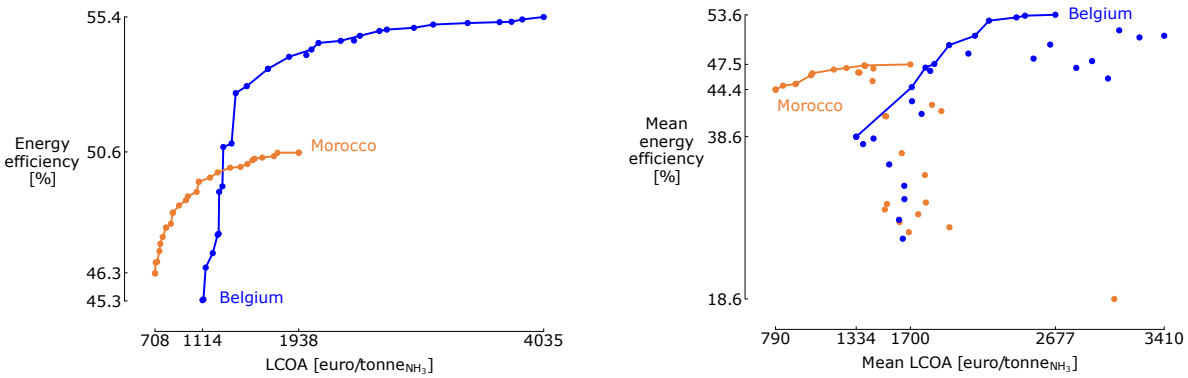

(a) Results of deterministic design optimization

(b) Results of robust design optimization

Figure 3: Deterministic and robust design optimization of PV-PtA plant of the Belgian and Moroccan case where maximizing the energy efficiency and minimizing levelized cost of ammonia results in a trade-off.

The robust design optimization shows a similar Pareto front between maximizing the mean efficiency and minimizing the mean levelized cost of ammonia (Figure 3b). In the RDO results, the Belgian case attains a higher mean energy efficiency (53.6%) than the Moroccan case (47.5%), but at a higher mean *LCOA* (2677 euro/tonne$_{NH_3}$ versus 1700 euro/tonne$_{NH_3}$). Still, the Moroccan plant achieve a lower *LCOA* at a higher efficiency (790 euro/tonne$_{NH_3}$ and 44.4%) than the Belgian plant (1334 euro/tonne$_{NH_3}$ at 38.6%). In addition to having the lowest LCOA, the Moroccan plant shows the smallest trade-off in standard deviation between the lowest mean *LCOA* and lowest standard deviation *LCOA* (Figure 5a). Between these extremes, there is a difference of 21 euro/tonne$_{NH_3}$ in standard deviation and 51 euro/tonne$_{NH_3}$ in mean. While for the Belgian case, there is a larger trade-off of 376 euro/tonne$_{NH_3}$ in mean *LCOA* and 92 euro/tonne$_{NH_3}$ in standard deviation. In terms of energy efficiency, we observe a small trade-off between the highest mean efficient and robust plant in the case of Belgium (5.71% difference in mean efficiency and 0.08% in standard deviation), where for Morocco, the trade-off is more significant in mean energy efficiency (29.3%) and standard deviation (1.05%).

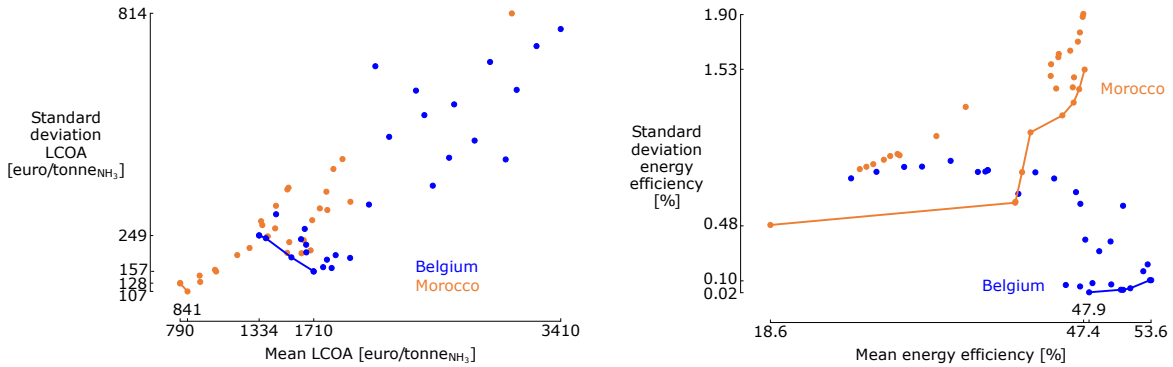

(a) Trade-off between mean and standard deviation LCOA

(b) Trade-off between mean and standard deviation energy efficiency

Figure 4: Pareto fronts of the mean and standard deviation of the *LCOA* and energy efficiency of the Belgian and Moroccan case.

We identified the PV and the PEM electrolyzer capacity as the two key design variables to obtain the Pareto fronts (Figure 5). In the best mean *LCOA* of the Morrocan case, the PV size is 2.38 times smaller in capacity than the best mean *LCOA* case of Belgium. This factor shows the impact of a renewable-rich location on a location with a lower yearly solar irradiance. For Belgium, the PV capacity goes towards the maximum boundary of 1 GWp to reach a smaller LCOA. In both cases, a lower PV capacity increases the mean *LCOA* (lower production of NH_3), but increases the mean efficiency. In addition, the PEM capacity is inversely proportional to the PV capacity, where a small PEM capacity provides for lower *LCOA* in both cases, while an increasing PEM capacity improves the mean energy efficiency of the PtA plant. This trend relates to the electrolyzer's efficiency, where the efficiency is the highest at lower loads. When the electrolyzer's load increases, its efficiency decreases to overpotential losses (Equation 3). In both cases, the electrolyzer capacity goes to the maximum set boundary of 1 GW to gain higher efficiency in the mean. For reaching the lowest standard deviation in energy efficiency, the PEM capacity needs to decrease (lower than the PV capacity), while the HBS and PSA capacities remain the same size in all designs. This observation implies that the most robust design (in energy efficiency) would require lower PEM capacities, therefore discarding larger quantities of excess solar energy, reducing the mean energy efficiency to increase its standard deviation (Equation 6). In addition to Morocco's PV and PEM capacities, we observe that the fuel cell capacity matches the HBS capacity at the lowest LCOA. To attain higher efficiencies, the fuel cell capacity increases while the capacity of the HBS does not increase. Like with the electrolyzer, the fuel cell system is more efficient when the system is oversized, which increases the capital expenses, but increases the energy efficiency of the PtA plant. In the case of Belgium, the fuel cell capacities remain below 0.04 kW. In addition, we observe that the minimal load of the NH_3 process lies between 10% and 11% for all designs in both cases. Therefore, this optimization shows the essential need for creating a Haber-Bosch process with lower operating loads to create an energy-efficient and cost-effective PtA plant. Therefore, the further development of a flexible Haber-Bosch is vital for the future application of these seasonal energy capture systems.

4. Conclusion

Technical and economic uncertainties have a significant impact on the Power-to-Ammonia process for capturing and storing seasonal renewable energy. Installing these storage systems in renewable-rich locations is cheaper than in locations with fewer renewables and high demand for electrofuels. In this paper, we modelled

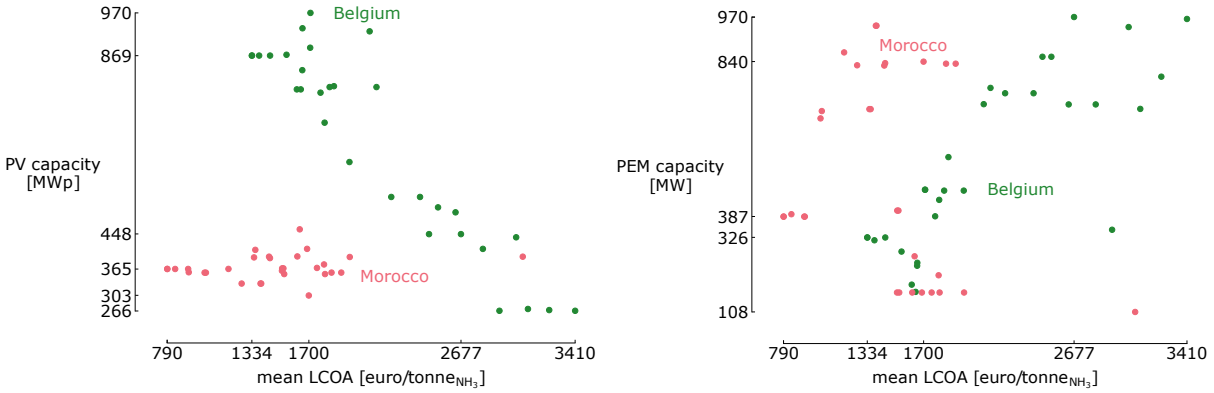

(a) TThe PV capacity influences the mean *LCOA* in the Belgian case.

(b) The PEM capacity impacts the mean *LCOA* in the Belgian and Moroccan case.

Figure 5: The PV and PEM capacities impacts the mean *LCOA* of the Belgian and Moroccan cases.

all the components to transform solar energy into ammonia, where we optimized the efficiency and levelized cost of this plant with robust design optimization. The results of the RDO on the PtA plant showed that the location in Morocco provides the lowest mean cost (between 790 euro/tonne$_{NH_3}$ and 841 euro/tonne$_{NH_3}$) and least sensitive designs (between 128 euro/tonne$_{NH_3}$ and 107 euro/tonne$_{NH_3}$) to the implemented uncertainties. In the case of Belgium this trade-off is significantly larger (between 1334 euro/tonne$_{NH_3}$ and 1710 euro/tonne$_{NH_3}$ in mean and between 249 euro/tonne$_{NH_3}$ and 157 euro/tonne$_{NH_3}$ in standard deviation). This large gap between the two cases originates from two design variables: the PV array's size and the PEM electrolyzer capacity combined with the more effective solar irradiance. Meanwhile, the Belgium case provided us with a design with the highest mean efficiency (53.6%) and a design with the lowest sensitivity (0.02%) on the standard deviation than the Moroccan case (highest mean of 47.5% and lowest standard deviation of 0.48%) to the absence of a ship and fuel cell backup system. We observed that the Morrocan case attains lower PV capacity for lower *LCOA* than the Belgium case, where the PEM electrolyzer capacity influences the efficiency of the PtA plant in mean and standard deviation. Therefore, the Moroccan case shows that ammonia plants located in the solar-rich environment are cheaper (in mean and less sensitive to uncertainties) to produce and then transport the NH_3 to Belgium than producing it locally. In terms of efficiency, the Belgium case shows better performance in mean and standard deviation because of the absence of a fuel cell and ship while having a grid as a backup system. However, this grid is implemented with a fixed price, while the grid price is uncertain in reality. In the future, we will implement these uncertainties while also including wind power while adding an extra objective where we want to minimize the environmental impact of these plants.

References

[1] IEA (2019). *The Future of Hydrogen*. Paris,, 2019. doi: 10.1787/1e0514c4-en.

[2] Christoph Hank, André Sternberg, Nikolas Köppel, Marius Holst, Tom Smolinka, Achim Schaadt, Christopher Hebling, and Hans-Martin Henning. Energy efficiency and economic assessment of imported energy carriers based on renewable electricity. *Sustainable Energy & Fuels*, 4(5):2256–2273, may 2020. ISSN 2398-4902. doi: 10.1039/d0se00067a.

[3] Pauline Caumon, Miguel Lopez-Botet Zulueta, Jérémy Louyrette, Sandrine Albou, Cyril Bourasseau, and Christine Mansilla. Flexible hydrogen production implementation in the French power system: Expected impacts at the French and European levels. *Energy*, 81:556–562, mar 2015. ISSN 0360-5442. doi: 10.1016/J.ENERGY.2014.12.073.

[4] Jürgen Fuhrmann, Marlene Hülsebrock, and Ulrike Krewer. Energy Storage Based on Electrochemical Conversion of Ammonia. In *Transition to Renewable Energy Systems*, pages 691–706. Wiley-VCH Verlag GmbH & Co. KGaA, Weinheim, Germany, jun 2013. ISBN 9783527673872. doi: 10.1002/9783527673872.ch33.

[5] Agustin. Valera-Medina and Rene. Banares-alcantara. *Techno-economic Challenges of green ammonia as an energy carrier*. Academic Press, 2021. ISBN 978-0-12-820560-0. doi: 10.1016/c2019-0-01417-3.

[6] Nicholas Salmon and René Bañares-Alcántara. Green ammonia as a spatial energy vector: a review. *Sustainable Energy & Fuels*, 5(11):2814–2839, jun 2021. doi: 10.1039/d1se00345c.

[7] Belgium. Belgium's Integrated National Energy and Climate Plan [B], 2018.

[8] Chris Peeters. Elia ' s view on Belgium ' s Energy Vision for 2050. (June):1–22, 2017. URL https://www.elia.be/{~}/media/files/Elia/publications-2/Rapports/Elia-view-on-Belgium-Energy-Vision-for-2050-EN.pdf.

[9] Gauthier Limpens and Hervé Jeanmart. Electricity storage needs for the energy transition: An EROI based analysis illustrated by the case of Belgium. *Energy*, 152:960–973, jun 2018. ISSN 03605442. doi: 10.1016/j.energy.2018.03.180.

[10] Hydrogen Import Coalition. Shipping sun and wind to Belgium is key in climate neutral economy Hydrogen Import Coalition. Technical report, Waterstofnet, 2021. URL https://beslissingenvlaamseregering.vlaanderen.be/document-view/5FAD539C20B6670008000274.

[11] Institute for Sustainable Process Technology and ISPT. Power to Ammonia. Technical report, ISPT, 2017. URL http://www.ispt.eu/media/ISPT-P2A-Final-Report.pdfhttp://www.ispt.eu/media/ISPT-P2A-Final-Report.pdf.

[12] Executive Hydrogen Import Coalition. Shipping sun and wind to Belgium is key in climate neutral economy. Technical report. URL https://beslissingenvlaamseregering.vlaanderen.be/document-view/5FAD539C20B6670008000274.

[13] Max. Appl. Ammonia : Principles and Industrial Practice. pages 0–3, 1996. ISSN 0048-3664. doi: 10.1002/pauz.19970260615.

[14] Collin Smith, Alfred K. Hill, and Laura Torrente-Murciano. Current and future role of Haber–Bosch ammonia in a carbon-free energy landscape. *Energy & Environmental Science*, 13(2):331–344, feb 2020. ISSN 1754-5692. doi: 10.1039/c9ee02873k.

[15] Cédric Philibert. Producing ammonia and fertilizers: new opportunities from renewables. *IEA Report*, pages 1–6, 2017. URL http://www.ee.co.za/wp-content/uploads/2017/06/Producing-ammonia-and-fertilizers-new-opportunities-from-renewables.pdf.

[16] Merve Ozturk and Ibrahim Dincer. An integrated system for ammonia production from renewable hydrogen: A case study. *International Journal of Hydrogen Energy*, 46(8):5918–5925, jan 2021. ISSN 03603199. doi: 10.1016/j.ijhydene.2019.12.127.

[17] Richard Michael Nayak-Luke and René Bañ ares Alcá ntara. Techno-economic viability of islanded green ammonia as a carbon-free energy vector and as a substitute for conventional production. *Cite this: Energy Environ. Sci*, 13:2957, 2020. doi: 10.1039/d0ee01707h.

[18] Julien Armijo and Cédric Philibert. Flexible production of green hydrogen and ammonia from variable solar and wind energy: Case study of Chile and Argentina. *International Journal of Hydrogen Energy*, 45 (3):1541–1558, jan 2020. ISSN 03603199. doi: 10.1016/j.ijhydene.2019.11.028.

[19] Ostuni. Method for load regulation of an ammonia plant, 2008. ISSN 00218979. URL https://patents.google.com/patent/US9463983B2/en.

[20] Izzat Iqbal Cheema and Ulrike Krewer. Optimisation of the Autothermal NH3 Production Process for Power-to-Ammonia. *Processes*, 8(1):38, dec 2019. ISSN 2227-9717. doi: 10.3390/pr8010038.

[21] Izzat Iqbal Cheema and Ulrike Krewer. Operating envelope of Haber–Bosch process design for power-to-ammonia. *RSC Advances*, 8(61):34926–34936, 2018. doi: 10.1039/C8RA06821F.

[22] S. Schulte Beerbühl, M. Fröhling, and F. Schultmann. Combined scheduling and capacity planning of electricity-based ammonia production to integrate renewable energies. *European Journal of Operational Research*, 241(3):851–862, mar 2015. ISSN 0377-2217. doi: 10.1016/J.EJOR.2014.08.039.

[23] Richard Nayak-Luke, René Bañares-Alcántara, and Ian Wilkinson. "Green" Ammonia: Impact of Renewable Energy Intermittency on Plant Sizing and Levelized Cost of Ammonia. *Industrial & Engineering Chemistry Research*, 57(43):14607–14616, oct 2018. ISSN 0888-5885. doi: 10.1021/acs.iecr.8b02447.

[24] Matthew J. Palys and Prodromos Daoutidis. Using hydrogen and ammonia for renewable energy storage: A geographically comprehensive techno-economic study. *Computers and Chemical Engineering*, 136:106785, may 2020. ISSN 00981354. doi: 10.1016/j.compchemeng.2020.106785.

[25] Matthew J. Palys, Hanchu Wang, Qi Zhang, and Prodromos Daoutidis. Renewable ammonia for sustainable energy and agriculture: vision and systems engineering opportunities, mar 2021. ISSN 22113398.

[26] William F Holmgren, Clifford W Hansen, and Mark A Mikofski. pvlib python: a python package for modeling solar energy systems. *The Journal of Open Source Software*, 3:884, 2018.

[27] Tafadzwa Gurupira and Arnold Rix. Pv simulation software comparisons: Pvsyst, nrel sam and pvlib. In *Conf.: SAUPEC*, 2017.

[28] Diederik Coppitters, Ward De Paepe, and Francesco Contino. Robust design optimization of a photovoltaic-battery-heat pump system with thermal storage under aleatory and epistemic uncertainty. *Energy*, 229:120692, aug 2021. ISSN 0360-5442. doi: 10.1016/J.ENERGY.2021.120692.

[29] Sunpower. *X-Series residential solar panels: supplementary technical specifications*.

[30] Alexander Buttler and Hartmut Spliethoff. Current status of water electrolysis for energy storage, grid balancing and sector coupling via power-to-gas and power-to-liquids: A review. *Renewable and Sustainable Energy Reviews*, 82:2440–2454, 2018. ISSN 18790690.

[31] Z. Abdin, C. J. Webb, and E. Maca Gray. Modelling and simulation of a proton exchange membrane (PEM) electrolyser cell. *International Journal of Hydrogen Energy*, 40(39):13243–13257, oct 2015. ISSN 03603199. doi: 10.1016/j.ijhydene.2015.07.129.

[32] Yu Wang, Julia Kowal, Matthias Leuthold, and Dirk Uwe Sauer. Storage system of renewable energy generated hydrogen for chemical industry Selection and/or peer-review under responsibility of Canadian Hydrogen and Fuel Cell Association. *Energy Procedia*, 29:657–667, 2012. doi: 10.1016/j.egypro.2012.09.076.

[33] S Ivanova and Robert Lewis. Producing Nitrogen via Pressure Swing Adsorption. *Progress, R Lewis - Chemical Engineering 2012, Undefined*, (June):38–42, 2012. URL `http://www.airproducts.com/products/gases/supply-options/onsite-gas-generation/{~}/media/ED77CF85C5EF40119FD964535E80E4D2.pdf`.

[34] Antonio Sánchez and Mariano Martín. Scale up and scale down issues of renewable ammonia plants: Towards modular design. *Sustainable Production and Consumption*, 16:176–192, oct 2018. ISSN 2352-5509. doi: 10.1016/J.SPC.2018.08.001.

[35] Alon Grinberg Dana, Oren Elishav, André Bardow, Gennady E. Shter, and Gideon S. Grader. Nitrogen-Based Fuels: A Power-to-Fuel-to-Power Analysis, jul 2016. ISSN 15213773.

[36] Eric R Morgan. *Techno-Economic Feasibility Study of Ammonia Plants Powered by Offshore Wind*. PhD thesis, feb 2013.

[37] Mahdi Fasihi, Robert Weiss, Jouni Savolainen, and Christian Breyer. Global potential of green ammonia based on hybrid PV-wind power plants. *Applied Energy*, 294:116170, apr 2021. ISSN 03062619. doi: 10.1016/j.apenergy.2020.116170.

[38] Matthew J. Palys, Anatoliy Kuznetsov, Joel Tallaksen, Michael Reese, and Prodromos Daoutidis. A novel system for ammonia-based sustainable energy and agriculture: Concept and design optimization. *Chemical Engineering and Processing - Process Intensification*, 140:11–21, jun 2019. ISSN 0255-2701. doi: 10.1016/J.CEP.2019.04.005.

[39] Karthik Murugesan and Vijayachitra Senniappan. Investigation of water management dynamics on the performance of a Ballard-Mark-V proton exchange membrane fuel cell stack system. *Int. J. Electrochem. Sci*, 8:7885–7904, 2013.

[40] Kyunghwa Kim, Gilltae Roh, Wook Kim, and Kangwoo Chun. A Preliminary Study on an Alternative Ship Propulsion System Fueled by Ammonia: Environmental and Economic Assessments. *Journal of Marine Science and Engineering*, 8(3):183, mar 2020. ISSN 2077-1312. doi: 10.3390/jmse8030183.

[41] shiptraffic.net. Sea distance calculator. URL `http://www.shiptraffic.net/2001/05/sea-distances-calculator.html`.

[42] Gelaro et al. renewables.ninja, 2017. URL `doi:10.1175/JCLI-D-16-0758.1`.

[43] Behnam Zakeri and Sanna Syri. Electrical energy storage systems: A comparative life cycle cost analysis. *Renewable and Sustainable Energy Reviews*, 42:569–596, 2015. ISSN 18790690. doi: 10.1016/J.RSER.2014.10.011.

[44] Diederik Coppitters, Ward De Paepe, and Francesco Contino. Robust design optimization and stochastic performance analysis of a grid-connected photovoltaic system with battery storage and hydrogen storage. *Energy*, 213:118798, dec 2020. ISSN 03605442. doi: 10.1016/j.energy.2020.118798.

[45] Thomas Huld, Richard Müller, and Attilio Gambardella. A new solar radiation database for estimating PV performance in Europe and Africa. *Solar Energy*, 86(6):1803–1815, jun 2012. ISSN 0038092X. doi: 10.1016/J.SOLENER.2012.03.006.

[46] C. Fúnez Guerra, L. Reyes-Bozo, E. Vyhmeister, M. Jaén Caparrós, José Luis Salazar, and C. Clemente-Jul. Technical-economic analysis for a green ammonia production plant in Chile and its subsequent transport to Japan. *Renewable Energy*, 157:404–414, sep 2020. ISSN 0960-1481. doi: 10.1016/J.RENENE.2020.05.041.

[47] Jussi Ikäheimo, Juha Kiviluoma, Robert Weiss, and Hannele Holttinen. Power-to-ammonia in future North European 100 % renewable power and heat system. *International Journal of Hydrogen Energy*, 43(36):17295–17308, sep 2018. ISSN 03603199. doi: 10.1016/j.ijhydene.2018.06.121.

[48] Jachin Gorre, Fabian Ruoss, Hannu Karjunen, Johannes Schaffert, and Tero Tynjälä. Cost benefits of optimizing hydrogen storage and methanation capacities for Power-to-Gas plants in dynamic operation. *Applied Energy*, 257:113967, jan 2020. ISSN 0306-2619. doi: 10.1016/J.APENERGY.2019.113967.

[49] Kevin Verleysen, Diederik Coppitters, Alessandro Parente, Ward De Paepe, Francesco Contino, Alessandro Parente, and Francesco Contino. How can power-to-ammonia be robust? Optimization of an ammonia synthesis plant powered by a wind turbine considering operational uncertainties. *Fuel*, 266:117049, apr 2019. ISSN 00162361. doi: 10.1016/j.fuel.2020.117049.

[50] Diederik Coppitters, Kevin Verleysen, Ward De Paepe, and Francesco Contino. How can renewable hydrogen compete with diesel in public transport? Robust design optimization of a hydrogen refueling station under techno-economic and environmental uncertainty. *Applied Energy*, 312:118694, apr 2022. ISSN 0306-2619. doi: 10.1016/J.APENERGY.2022.118694.

[51] P. Laššák, J. Labovský, and Ĺ. Jelemenský. Influence of parameter uncertainty on modeling of industrial ammonia reactor for safety and operability analysis. *Journal of Loss Prevention in the Process Industries*, 23(2):280–288, mar 2010. ISSN 0950-4230. doi: 10.1016/J.JLP.2009.10.001.

[52] Yiwei Qiu, Jin Lin, Xiaoshuang Chen, Feng Liu, and Yonghua Song. Nonintrusive Uncertainty Quantification of Dynamic Power Systems Subject to Stochastic Excitations. 2020. doi: 10.1109/tpwrs.2020.3007746.

[53] E. Torre, S. Marelli, P. Embrechts, and B. Sudret. Data-driven polynomial chaos expansion for machine learning regression. *Journal of Computational Physics*, 388:601–623, aug 2018. doi: 10.1016/j.jcp.2019.03.039.

[54] Géraud Blatman and Bruno Sudret. Sparse polynomial chaos expansions and adaptive stochastic finite elements using a regression approach. *Comptes Rendus - Mecanique*, 336(6):518–523, jun 2008. ISSN 16310721. doi: 10.1016/j.crme.2008.02.013.